World Journal of Advanced Research and Reviews
eISSN: 2581-9615 CODEN (USA): WJARAI
Cross Ref DOI: 10.30574/wjarr
Journal homepage: https://wjarr.com/

(Research Article)

Check for updates

Petrographic and geochemical characterization of the Parawi bauxitic deposit, Republic of Guinea

Mohamed Samuel Moriah Conte *, Abdoulaye Kadiatou Diallo, Aly Soumah, Mohamed Lamine Timite, Mohamed Fofana and Djibril M'Mamy Camara

Applied Research Laboratory in Geosciences and Environment, Fundamental Geology and Prospecting Research Unit (URGFP), Department of Geological Services, Higher Institute of Mines and Geology of Boké (ISMGB), Baralande-Prefecture Boke, BP: 84 Boké.

World Journal of Advanced Research and Reviews, 2025, 28(01), 1181-1197

Publication history: Received on 02 September 2025; revised on 12 October 2025; accepted on 14 October 2025

Article DOI: https://doi.org/10.30574/wjarr.2025.28.1.3491

Abstract

Global population growth leads to a high demand for quality minerals, particularly for industrial production. Guinea, rich in mineral resources, has more than 23 billion tonnes of bauxite in the Boké region, of which the sub-prefecture of Sangarédi, operated by the Compagnie des Bauxites de Guinée (CBG), is a major site. In this context, a geological characterization study of the Parawi bauxitic deposit was carried out to better understand its petrographic, mineralogical and geochemical composition.

The methodology adopted is based on a geological prospecting campaign, with samples collected in the field using an Estwing-type hammer, as well as in boreholes thanks to an ATLAS COPCO drilling rig. Petrographic analysis reveals that the deposit developed on Devonian aleurolites and argillites, intruded by Mesozoic dolerites, then topped with Cenozoic bauxites.

The semi-quantitative mineralogical study indicates a predominance of gibbsite (43–84%), followed by boehmite (1–20%). The contents of hematite and goethite-alumogoethite vary between 1 and 21%, while kaolinite and quartz remain marginal (0–1%). On the classification diagrams, the samples are divided between bauxite, ferritic bauxite and kaolinitic bauxite. The high Al2O3 contents reflect a strong lateritization, while the SiO2 contents reflect a weak weathering. Observed bauxitisation processes include kaolinite preservation or destruction, deferruginisation and dehydration.

This geological characterization is an essential step to ensure the profitability, safety and sustainability of the exploitation of the Parawi deposit, and guides decision-making at each phase of the mining project.

Keywords: Bauxite; Petrography; Mineralogy; Geochemistry

1. Introduction

The exploitation of mineral resources remains limited in many developing countries, due to the lack of scientific data on exploitable deposits. Among these resources, bauxites occupy a prominent place due to their aluminum wealth and their strategic importance in the industry. From a geological point of view, they appear in different forms (karst, sedimentary or lateritic) resulting from intense continental weathering processes [1]. Their genesis and facies are varied and subject to classifications based on mineralogy, chemical composition, geomorphology and the nature of the bedrock [2], [3].

* Corresponding author: Mohamed Samuel Moriah Conte

Copyright © 2025 Author(s) retain the copyright of this article. This article is published under the terms of the Creative Commons Attribution License 4.0.

Global bauxite production, estimated at 348 million tonnes in 2019, is growing by more than 5% per year, driven by strong Chinese demand. The main producers are Australia, Guinea, China, Brazil and India [4]. Guinea occupies a central place, with more than 40 billion tonnes of reserves, including 23 billion located in the Boké region [5]. The discovery of bauxite in Guinea dates back to 1819 by G. Mollien, but its industrial exploitation only really began in 1920 with the interest of the Société des Bauxites du Midi [6]. Since then, numerous studies have identified significant deposits, notably at Parawi [7], [8], [9], [10], [11], [12]. However, these studies mainly focus on general geology and resource assessment, without detailed analysis of petrography, mineralogy and geochemistry with modern methods.

at this time, the issue arises as follows: how an integrated study of the petrography, mineralogy and geochemistry of bauxite and their source rocks from the Parawi deposit can allow a better understanding of their genesis, to evaluate their potential and contribute to rational and sustainable exploitation in the CBG concession?

It is in this perspective that the present study, entitled "Geological characterization of the Parawi bauxitic deposit, Republic of Guinea". The general objective is to analyze in an integrated way the petrographic, mineralogical and geochemical characteristics of bauxites and their source rocks, in order to better understand their genesis and evolution. More specifically, it is about

- characterize the different bauxitic facies present on the Parawi plateau;
- analyze the mineralogical composition in order to identify the dominant and accessory phases;
- determine the chemical composition of the samples to evaluate the degree of lateritisation and the associated processes.

To achieve this, we will implement a methodological approach articulated in several steps. Initially, a geological prospecting campaign will be carried out to identify the bauxitic facies and to carry out representative sampling, both in outcrop and in drilling. In a second step, these samples will be subjected to petrographic and mineralogical analyses, allowing the description of the textures, structures and mineral composition of the bauxites. Finally, geochemical analyses will be conducted to determine the major oxide contents and evaluate the bauxitisation and lateritization processes that led to the development of the deposit.

This integrated approach should not only characterize the nature and quality of bauxite from the Parawi plateau, but also provide useful information for the valorization, planning and sustainability of mining in the CBG concession.

2. Geological setting

2.1. Geological context of the study region

The Prefecture of Boké is located in the northwest of Guinea, between latitudes 10°30' and 11°45' north, and longitudes 13°45' and 15° West (figure 1). It covers an area of 11,453 km 2. Administratively, it is bordered to the east and northeast by the prefectures of Télimélé and Gaoual, to the west by the Atlantic Ocean, and to the south by the prefecture of Boffa [13].

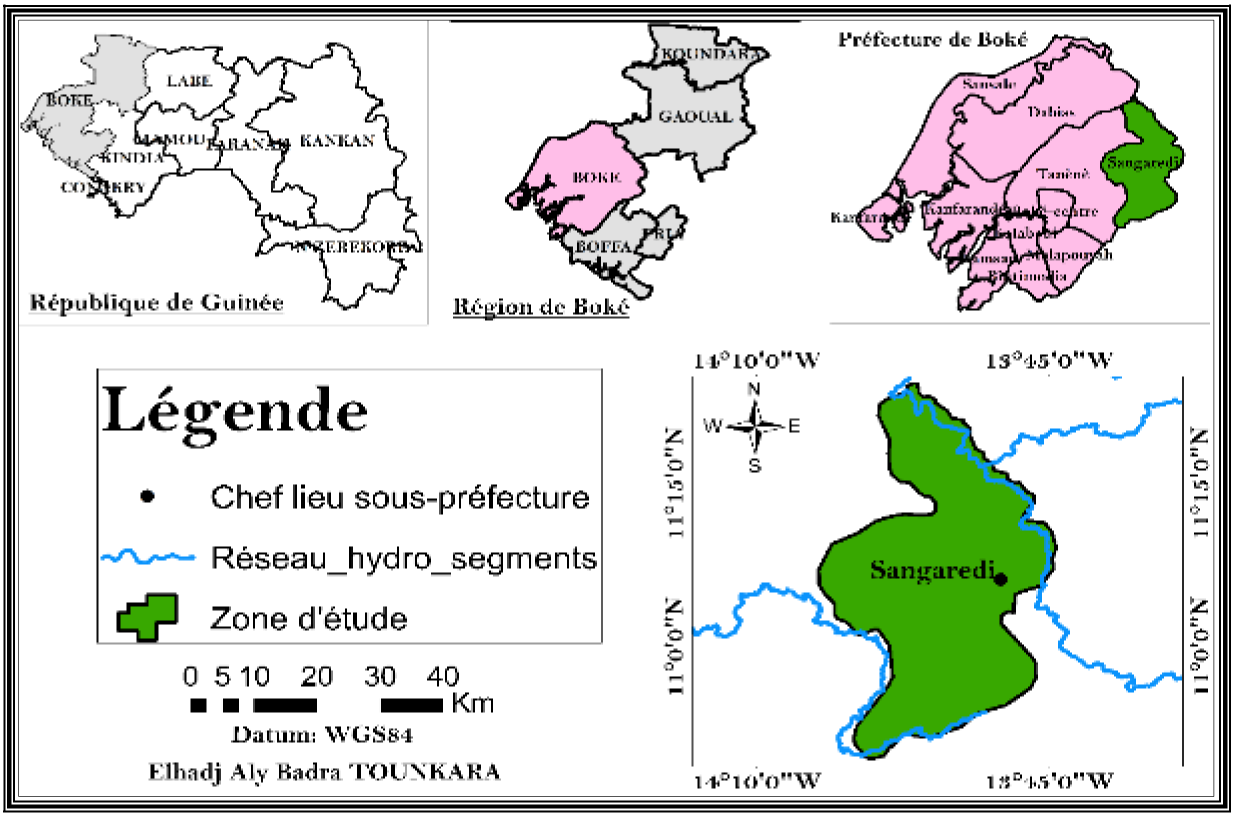

Figure 1 Map of the study region in Guinea

The studied region (Figure 2) presents a complex geological cover, consisting mainly of paleozoic sedimentary formations, intersected by mesozoic magmatic intrusions and surmounted by Cenozoic and quaternary formations. The Paleozoic series successively include the quartzose sandstones of the Ordovician (following Pita), the argillites and aleurolites of the Silurian (following Telimele), then the alternation of argillites and aleurolites of the Devonian (following Faro). The Cenozoic formations include, in the Palaeogene, marine deposits and lateritic crusts resulting from the alteration of sedimentary and intrusive rocks, and in the Neogene, pisolitic, clay, and gibbsic deposits locally reaching 30 m. The quaternary formations, as for them, are represented by marine, fluvial and continental deposits of variable thickness (2 to 5 m), extending into river valleys and coastal areas [7], [8], [9].

The magmatic history of the region is marked by intense activity during the Mesozoic, responsible for the intrusion of dolerites, gabbro-dolerites and Kongo-diabases. These magmatic bodies, dated from the Jurassic (147–167 Ma), appear as subhorizontal sills and more rarely as dykes. Their implementation was favored by the contact zones between argillites and Ordovician sandstones. The thickness of these intrusions is generally between 50 and 70 m, but may locally exceed 100 m, thus constituting important structural levels in the geological evolution of the zone [7], [8], [9].

Structurally, the region belongs to the Bowé Shield, located in the northwest of the Guinean-Liberian shield, in the southwest sector of the North African platform. This platform is represented by a sedimentary cover subdivided into two structural sub-stages. The whole reflects a geodynamic evolution marked by the alternation of sedimentary deposits, magmatic events and tectonic processes, which conditioned the establishment of current formations and the structuring of the regional basement [7], [8], [9].

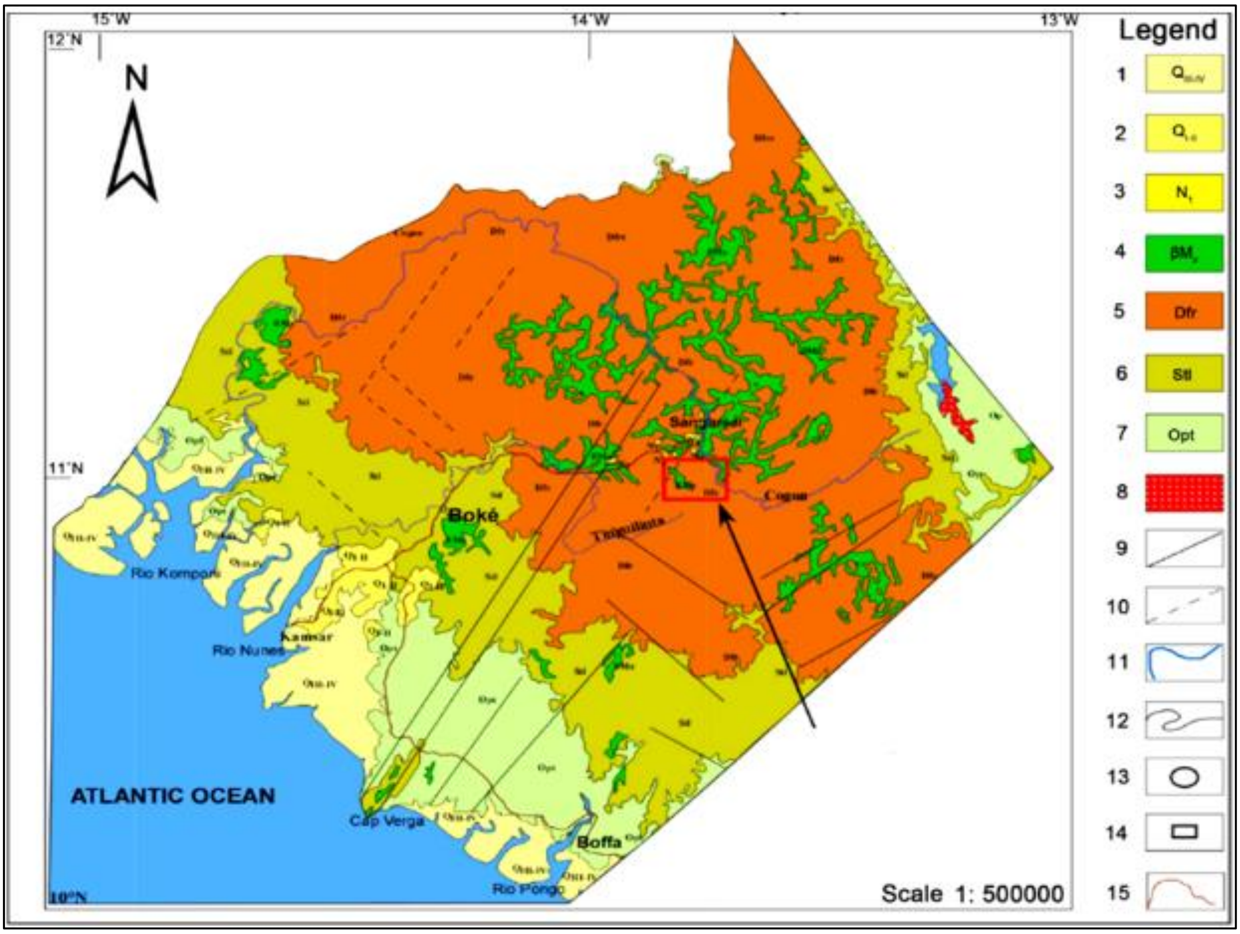

Figure 2 Geological map of the study region (Mamedov [7]; modify after)

1-Non-differentiated deposits: sandy and sandy rubbing lime with gravel, galets deleuvio-proluvionnaires ; 2-Non-differentiated deposits: clay sands and clay limon, sands, gra vels, aluvionnairs ; 3-Laterized rocks: sands, sandy limons, conglomerates ; 4-Mesozoic Dolerites ; 5-Devonian Faro Suite ; 6-Silurian Telemile suite ; 7-Ordovician Pita Suite ; 8-Granites and grand orates to biotitles ; 9-Bankruptcy Fails ; 10-Assorted Fails ; 11-Streams ; 12-Geological Limits Established ; 13-Cities ; 14-Deputy Prefecture ; 15-Roads.

2.2. Geology of the bauxitic deposit of Parawi

The results of the geological survey carried out from 1974 to 1976 on the Gaoual sheet at 1/200,000, with the assistance of Soviet geologists [8], made it possible to highlight the geological formations of the Parawi bauxitic plateau (Figure 3). According to Mamedov [8], these formations include the lower limb of the Faro suite (Dfr1), consisting of fine sandstones, aleuro-sandstones and lentils of aleurolites, associated with pseudomorphic bauxites and ferruginous laterites, as well as the upper limb of the Faro suite (Dfr2), composed of banded massive argilites, aleuro-argilites and bound aleurolites, with intercalations of fine sandstone. To these groups are added the quaternary deposits (QI and QIII-IV), located on the slopes of the Kéwéwol valley and in the valleys surrounding the bowes of the deposit, whose widths range from 50 to 400 meters, but with no alteration sequences at the bottom of the valleys [8], [9].

Structurally, the Parawi deposit has been affected by tectonic movements, resulting in fault bundles that intersect the multi-block deposit in all directions [13]. The magmatic history is marked by the intrusion of a basic trappic magma during the Mesozoic, forming dolerites in sills from a geomorphological point of view, the HALCO concession is located on the western slope of the Fouta-Djalon plateau. It is part of a series of plateaux bordered to the east by pre-Michaocene stratigraphic units and to the west by the Atlantic coastal plain, thus grouping several bauxitic plateaux [8], [9].

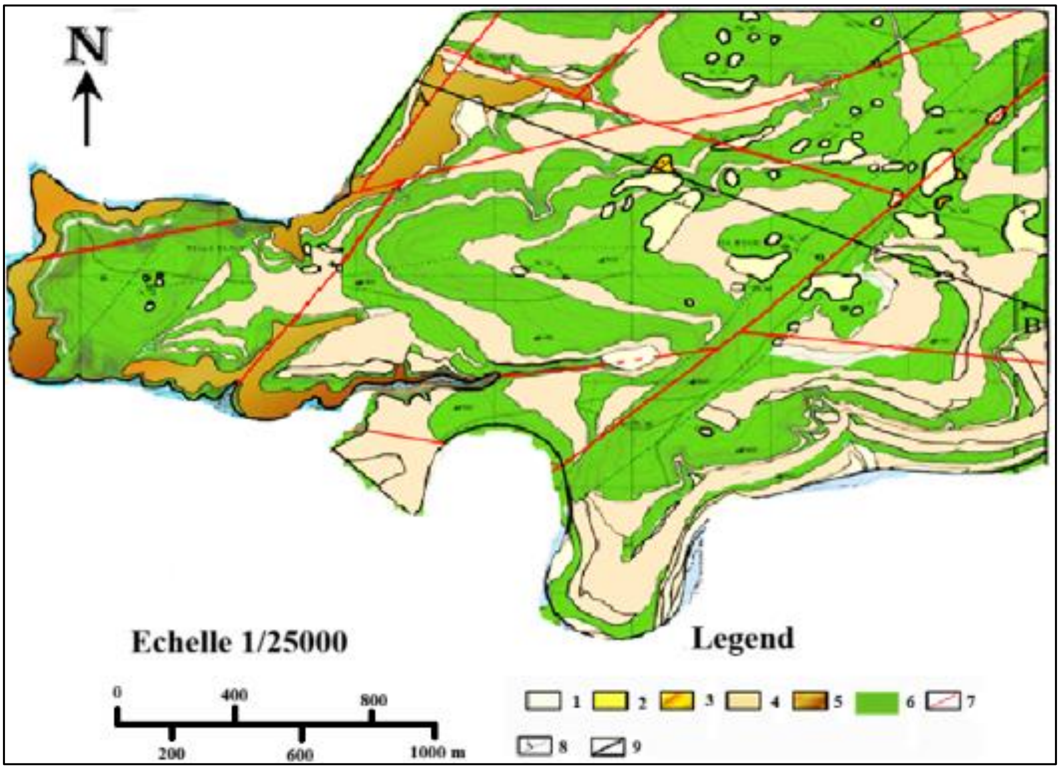

Figure 3 Geological map of the Parawi deposit [8]

1-Proluvio-Deluvial deposit of the high terraces; 2- Neogene system. Middle Miocene. Sangaredi series. Gravel, pebbles and sand, alluvial and alluvial-lacustrine, transformed into sedimentary lateritic bauxites (b- gravelly); 3- Neogene system. Middle Miocene. Sangaredi series. Gravels, pebbles and sand, alluvial and alluvial-lacustrine, transformed into sedimentary lateritic bauxites (a-conglomeratic); 4- Devonian System Faro Suite (upper limb) Argillite, aleulorite with rare sandstone interbeds; 5- Devonian System Faro Suite (lower limb) Argillite, aleulorite with rare sandstone interbeds; 6- Mesozoic intrusive rock (Dolerites); 7- Fissuring zones; 8- Bed shape of the deposits of the Sangaredi series; 9- Cut line A-B.

3. Materials and Methods

For the realization of this geological characterization study of the bauxitic deposit of Parawi, several materials were mobilized. In the field, the geologist’s hammer of the Estwing type was used for the sampling of flush samples, while a GPS GARMIN MAP 64s made it possible to georeference the sampling points. The mine compass was used to measure the direction of the dips, and the ATLAS COPCO drill rig was used for drilling from a depth of 8 to 12 m. In the laboratory, the petrographic study was conducted under a polarizing microscope using thin sections, and the geochemical composition was determined using ICP-OES spectrometry. The software Canvas (digitization of maps) and Triplot (creation of ternary diagrams) completed the analysis.

The methodology adopted combined several approaches. The literature search gathered previous scientific data on the geology of the area. A field campaign conducted from August 11 to September 11, 2023, as part of an internship at the Compagnie des Bauxites de Guinée (CBG), made it possible to collect samples at outcrop and in a drill hole, as well as to describe lithologically the cores to establish stratigraphic logs. In the laboratory, the samples were prepared, some for thin slides and others for mechanical and geochemical analyses. Finally, the processing and interpretation of geochemical results were carried out using binary and ternary diagrams, allowing a better understanding of the composition and evolution of the bauxites studied.

4. Results and discussion

4.1. Stratigraphic result

According to the data from exploratory drilling, the geological formations of the Parawi plateau (Figure 4) present a generally similar stratigraphic organization, characterized by four major groups: at the base, the bedrock, covered by a clay-ferruginous more or less thick, then a bauxitic horizon with varied facies, and finally the vegetable soil. However, the thickness and composition of these levels vary from one log to another. Thus, some drilling reveals a transition dominated by kaolinitic clays and ferruginous laterites, while others highlight the presence of red and yellow ferruplantites or gravelly conglomeratic bauxites deriving from the formations of the Sangaredi series. Similarly, the bauxitic horizons are distinguished by pseudomorphic, geomorphic or even strongly ferruginous facies, reflecting the diversity of lateritization and alteration processes that affected the area. This heterogeneity highlights the complexity of the geological evolution of the deposit and constitutes a key element for its characterization [2], [3].

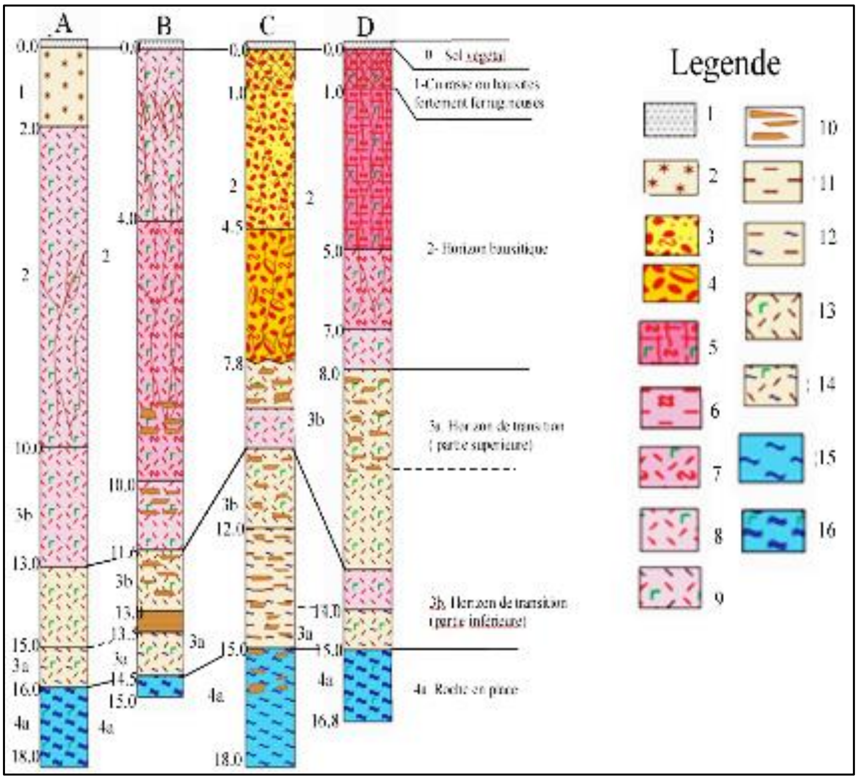

Figure 4 Stratigraphic logs of holes A, B, C and D [8]

1-Vegetable soil ; 2-Ferruginous laterites (cuirasses) ; 3-Gravelly and gravelly-sandstone bauxites ; 4-Gravelly-conglomeratic bauxites ; 5-Massive gelomorphic bauxites ; 6-Strongly gelled pseudomorphic bauxites derived from aleuro-argillites ; 7-Pseudomorphic gelled bauxites ; 8-Pseudomorphic classic lateritic bauxites ; 9-Low-quality pseudomorphic classic lateritic bauxites; 10-Red and tobacco-yellow ferriplantites ;11-Ferruginous laterites of the transition zone ; 12- Ferruginous laterites of the transition zone with clayey nests ; 13- Ferruginous laterites of the transition zone with clayey nests ; 14-White, grayish-white and pink kaolinitic clays ; 15-Versicolor kaolinitic clays ; 16-Polymineral kaolinite-montmorillonite clays derived from dolerites.

4.2. Petrographic result

The petrographic analysis of samples from the Parawi deposit highlights three main types of bauxite according to their formation mode (Figure 5). Lateritic in situ or residual bauxites, which represent about 75% of the CBG reserves, are formed directly by the alteration of Palaeozoic mother rocks (argillites and Devonian aleuro-argillites) and Mesozoic dolerites. They present themselves under various facies (structural, fragmentary, brecciated, skeletal) and are distinguished by their ribboned or massive textures. Then come the sedimentary lateritic bauxites, resulting from the accumulation of debris within the Sangarédi series, representing about 22% of the reserves. They are declined in gravelo-conglomeratic, conglomeratic, gravelly and gravelo-grésoid facies, generally poorly classified and characterized by embedded pebbles or lenses. Finally, the chemogenic bauxites, which result from recrystallization and alumina enrichment of pre-existing bauxite, represent only 3% of total reserves but include specific varieties such as the geomorphic bauxite (aphanitic and oolithic) and the gelated bauxites. The latter, recognizable by their light hues and micro-oolitic texture, are widespread in Parawi where they form nearly 63% of the resources of the deposit [8].

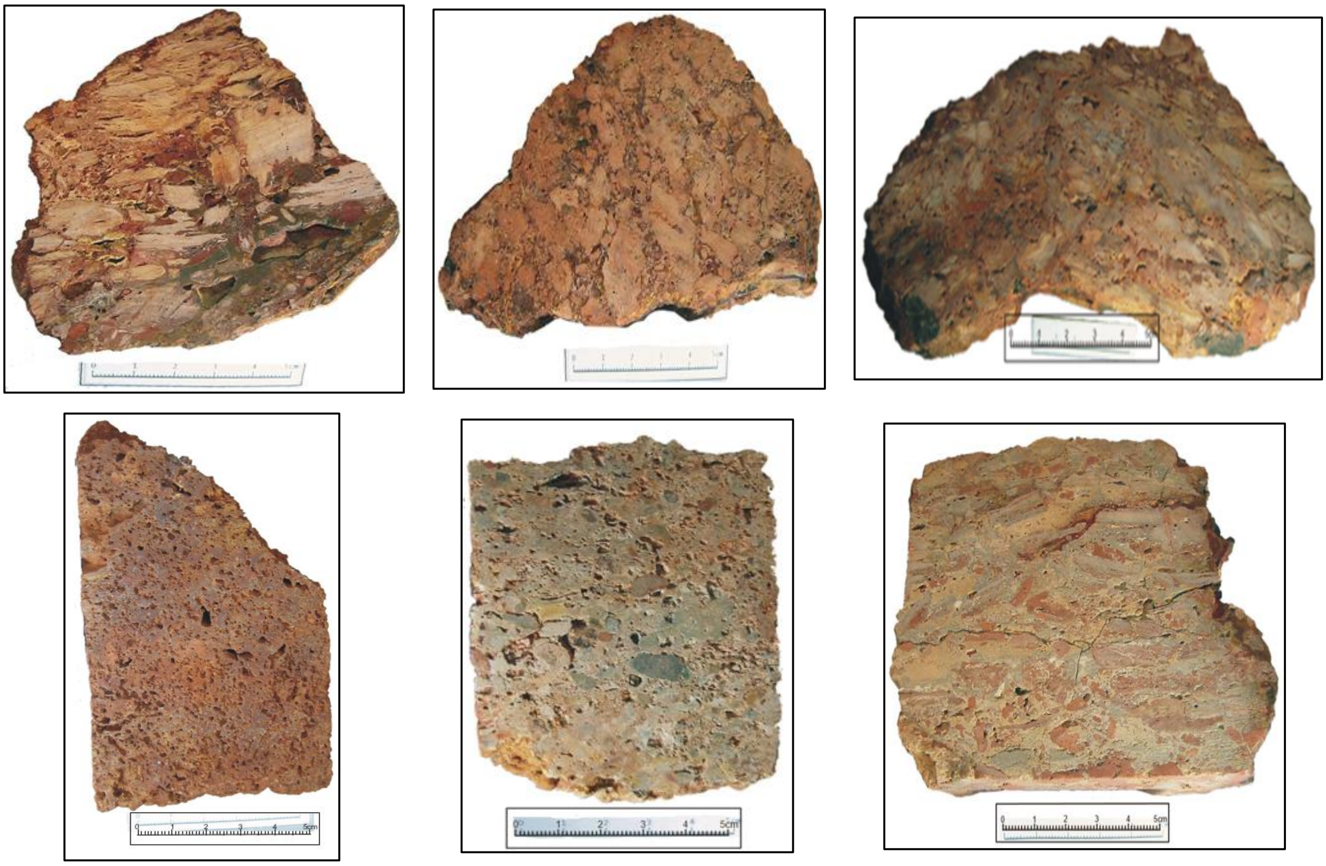

Figure 5 Lateritic classical bauxites in situ and chemogenic from Parawi

A -Ferruginous bauxite derived from aleuro-argillites; b -Ferruginous bauxite derived from argillites; c -Aluminous bauxite derived from aleurolites; d- Classical lateritic in situ bauxites derived from dolerites; e- Sedimentary bauxites (gravelly); b- Gelified bauxite derived from aleuro-argillites

Under the microscope, the bauxites from the Parawi deposit reveal a great diversity of structures and compositions according to their origin (Figure 6). Those deriving from the aleuro-argillites are weakly ferruginous, with fragments in various hues ranging from colorless to cherry red or red brown, and present a microcrystalline structure sometimes gelomorphic. Apodoleritic bauxites retain in places the ophitic design of the dolerites, the gibbsite forming aggregates surrounded by plagioclase, while the dark minerals are replaced by a gibbsite-goethitic matrix enriched with iron. Sedimentary bauxites have a very fine basal cement, often pink and highly porous (30–50%), sometimes replaced by a gelomorphic or microoolitic substance, with well-marked concentric structures in the ooliths, intersected with gibbsite veinlets. In oolitic varieties, the cement is rather amorphous or cryptocrystalline. Finally, in apodoleritic and structural gelled bauxites, gelation results in the formation of gibbsic and boehmitic nests or veinules, giving the rocks a micro- to finely crystalline texture while disrupting inherited structures [8].

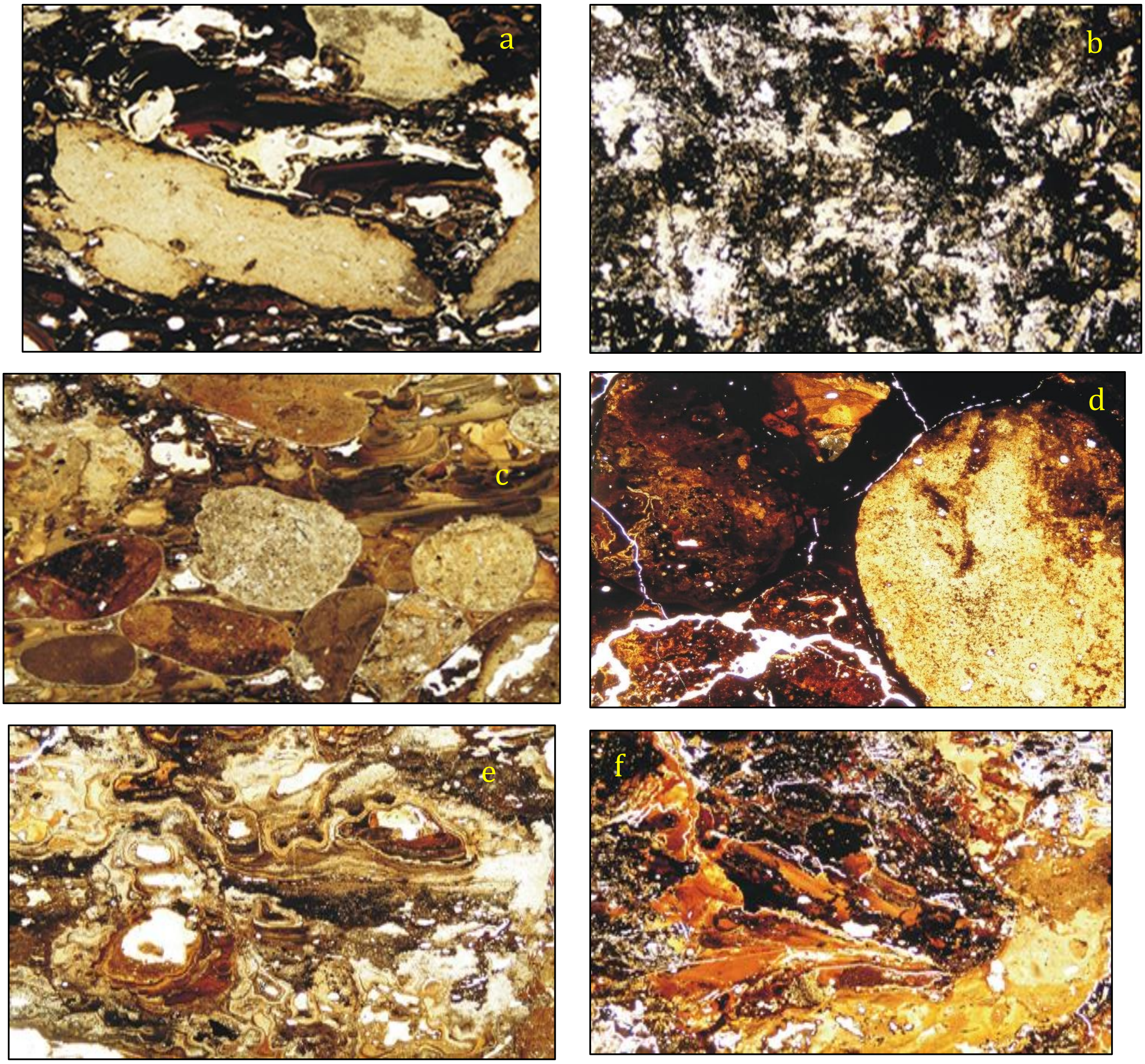

A-Aleuro-argillite bauxite; b- Apodoleritic lateritic bauxite; c- Gravelly bauxite; d- Oolithic bauxite; e- Gelled bauxite; f- Gemolmorphic bauxite.

Figure 6 Miscrocopic observation of bauxite samples from Parawi LPNA

4.3. Mineralogical result

The semi-quantitative mineralogical analysis reveals that the bauxites from the Parawi deposit are mainly composed of gibbsite [Al (OH)], with proportions varying from 43 to 84%. Boehmite [AlO (OH)] is also present but in smaller quantities, ranging from 1 to 20%. The ferruginous minerals, represented by hematite and goethite-alumogoethite, total between 1 and 21% of the composition. Finally, kaolinite [$Al_2Si_2O_5(OH)_4$] and quartz [SiO_2] appear in very low proportions, generally less than 1% (Table 1).

Table 1 Estimated mineral abundance of the Parawi bauxite deposits

Mineralogical composition in percentage %	Chemical Formula	Residual bauxite		Sedimentary bauxite		Chimogene bauxite		
Gibbsite	$Al(OH)_3$	43	60	59	84	52	53	84
Boehmite	Al (OH)	0	2	4	20	1	5	10
Goethite-alumogoethite	$(Fe_3+Al)O(OH)$	2	13	1	6	5	16	2
Hématite	Fe_2O_3	8	21	1	5	8	5	1
kaolinite	$Al_2Si_2O_5(OH)_4$	0	1	0	1	0	1	-
Quartz	SiO_2	0	1	0	1	0	1	-
Phase amorphe aux rayon X		8	41	0	27	0	5	25

4.4. Géochimical results

The geochemical analysis of major elements carried out on fifty (50) samples from 16 boreholes in the Parawi bauxitic plateau (Table 2) highlights a notable variability in composition. The alumina content (Al_2O_3) varies between 45.1% (sample PrwBF070 from borehole PrwBF07) and 53.92% (sample PrwBF090 from borehole PrwBF09). Silicon dioxide (SiO_2)) ranges from 1.43% (sample PrwBF090 from borehole PrwBF09) to 2.8% (sample PrwBF011 from borehole PrwBF01). Iron oxide (Fe_2O_3)) exhibits values ranging from 12.39% (sample PrwBF161 from borehole PrwBF16) to 26.6% (sample PrwBF010 from borehole PrwBF01). Titanium oxide (TiO_2), on the other hand, fluctuates between 0.77% (sample PrwBF052 from borehole PrwBF05) and 3.95% (sample PrwBF145 from borehole PrwBF14). Finally, the loss on ignition (LOI), indicative of bound water and volatile matter content, ranges from 23.22% (sample PrwBF100 from borehole PrwBF10) to 29.07% (sample PrwBF161 from borehole PrwBF16).

Table 2 Results of geochemical analyses

Forage	Echantillons	From	to	Al_2O_3	SiO_2	Fe_2O_3	TiO_2	LOI
PrwBF01	Prw BF010	1	2	45,4	2,2	26,6	0,9	23,99
	Prw BF011	2	3	49,2	2,8	19,3	0,95	27,05
	Prw BF012	3	4	48,1	2,57	21,6	1,16	25,86
	Prw BF013	4	5	49,2	2,5	19,8	0,89	26,87
	Prw BF014	5	6	46,5	2,2	24,1	1,11	25,33
PrwBF02	PrwBF020	1	2	45,3	2,02	24,6	2,13	25,13
	PrwBF021	2	3	45,7	2,09	24,2	1,66	25,55
PrwBF03	PrwBF030	0	1	46,3	2,37	21,8	2,34	26,46
	PrwBF031	1	2	45,7	2,6	22,4	2,36	26,22
	PrwBF032	2	3	45,8	2,45	23,1	2,2	25,7
	PrwBF033	3	4	47,5	2,29	20,8	2,08	26,71
	PrwBF034	4	5	47,7	2,34	20,4	1,83	27,14
	PrwBF035	5	6	49,9	2,05	18,1	1,48	27,79
PrwBF04	PrwBF040	2	3	47,3	1,92	22,4	1,03	26,64
	PrwBF041	3	4	50,6	2,25	17,6	1,06	27,78
	PrwBF042	4	5	49,4	2,19	19	1,56	27,16
	PrwBF043	5	6	47,6	1,95	22	1,89	25,86

PrwBF05	PrwBF050	1	2	50,6	1,99	17,4	1,56	27,89
	PrwBF051	2	3	49,6	2,2	18,7	1,26	27,55
	PrwBF052	3	4	50,7	2,16	17,9	0,77	27,89
PrwBF06	PrwBF060	0	1	47,36	1,62	23,01	1,83	25,76
PrwBF07	PrwBF070	0,3	1	45,1	2,09	24,7	1,84	25,54
	PrwBF071	1	2	46,3	2,21	23,8	1,53	25,52
PrwBF08	PrwBF080	4	5	46,19	1,54	25,54	1,28	24,36
PrwBF09	PrwBF090	2	3	53,92	1,43	15,83	2,19	24,97
	PrwBF091	3	4	51,25	1,46	15,93	2,84	26,78
PrwBF10	PrwBF100	2	3	45,61	2,76	24,19	3,51	23,22
	PrwBF101	3	4	46,76	2,54	22,96	3,66	23,47
	PrwBF102	4	5	46,78	2,61	23,24	3,2	23,56
	PrwBF103	5	6	49,17	2,36	19,11	3,71	25,05
	PrwBF104	6	7	50,18	2,35	17,29	3,55	26,1
	PrwBF105	7	8	47,42	2,29	20,79	3,75	25,2
PrwBF11	PrwBF110	0	1	46,17	2,17	23,95	2,46	24,69
	PrwBF111	1	2	45,79	2,16	23,2	3,39	24,93
PrwBF12	PrwBF120	3	4	48,3	1,7	20,6	1,92	26,58
PrwBF13	PrwBF130	3	4	51,8	1,88	14,7	2,75	28,2
	PrwBF131	4	5	47,2	1,74	21	3,39	25,98
PrwBF14	PrwBF140	1	2	48	2,42	22	1,91	25,04
	PrwBF141	2	3	49,4	2,25	19,9	1,51	26,28
	PrwBF142	3	4	49,1	2,23	19,8	2,15	26,12
	PrwBF143	4	5	49,2	2,22	18,7	3,17	26,08
	PrwBF144	5	6	52,1	1,9	15,5	2,36	27,68
	PrwBF145	6	7	49,5	1,99	17,8	3,95	26,21
	PrwBF146	7	8	48,7	1,61	20,7	1,88	26,51
PrwBF15	PrwBF150	0	1	53,31	2,32	13,91	2,01	26,55
	PrwBF151	1	2	47,77	1,87	22,31	1,46	24,67
	PrwBF152	2	3	46,97	1,89	22,98	1,39	24,98
PrwBF16	PrwBF160	1	2	50,79	2,37	16,77	1,08	27,35
	PrwBF161	2	3	53,65	2,43	12,39	0,79	29,07
	PrwBF162	3	4	49,31	2,08	18,58	1,95	26,72

The mineralogical classification according to Aleva [14] applied to samples from the Parawi plateau highlights a clear predominance of bauxitic facies. Indeed, the sample PrwBF111 falls into the bauxitic field (area 1); the samples PrwBF131, PrwBF042, PrwBF043, and PrwBF140 fall into the kaolinitic bauxite fields (zones 2 and 3), which indicates a more marked influence of silica; the samples PrwBF012, PrwBF021, PrwBF030, PrwBF032, PrwBF070, PrwBF160 fall into the laterite field (area 6) reflecting extensive alteration with ferruginous enrichment; samples PrwBF033, PrwBF034, PrwBF040, PrwBF041, PrwBF050, PrwBF52, PrwBF130, PrwBF140, PrwBF143, PrwBF145 and PrwBF146 fall into the bauxite field (area 7); samples PrwBF010, PrwBF031, PrwBF051, PrwBF080, PrwBF100, PrwBF101, PrwBF102, PrwBF104, PrwBF105, PrwBF110, PrwBF120, PrwBF150, PrwBF152, PrwBF161 fall into the ferritic bauxite field (area 8) whose content is high in iron (Figure 7).

Overall, the distribution of samples on the diagram reflects a bauxitic dominance within the Parawi deposit, but with localized lateritic and kaolinitic transitions. This variability illustrates the diversity of weathering processes and geochemical trajectories that led to the establishment of the lateritic profile [2], [3], [11], [15], [16], [17], [18].

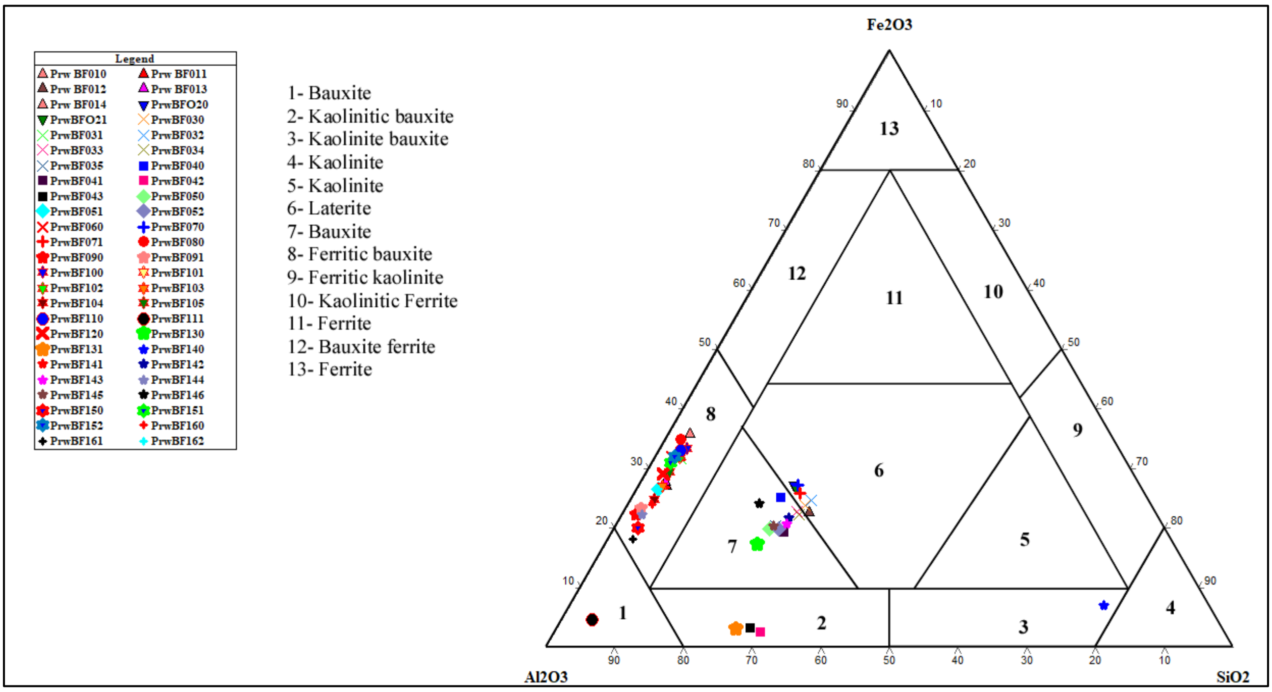

Figure 7 Triangular diagram between Al2O3-Fe2O3-SiO2 after Aleva [14]

The triangular diagram of the degree of laterization according to Schellmann [19] shows that the sample PrwBF140 falls into the field of kaolinization; then the samples PrwBF012, PrwBF032, PrwBF042, PrwBF043 localize in the field of moderate laterization and finally, the rest of the samples from the Parawi plateau (PrwBF010, PrwBF011, PrwBF013, PrwBF014, PrwBF06, PrwBF07, PrwBF08, PrwBF09, PrwBF10, PrwBF11, PrwBF12, PrwBF13, PrwBF14, PrwBF15 and PrwBF16) clearly cluster in the field of strong lateritisation. This position reflects a very high degree of alteration, marked by a strong enrichment in Al_2O_3 and Fe_2O_3, accompanied by an intense leaching of silica (Figure 8).

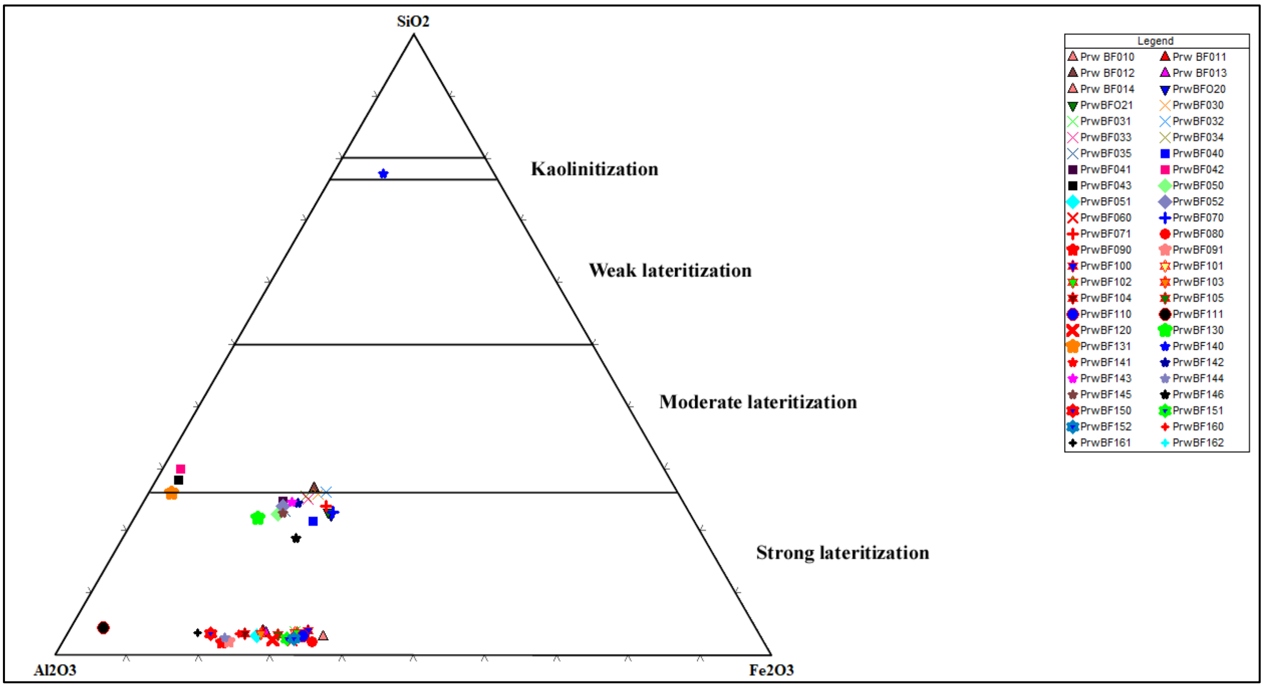

Figure 8 Triangular diagram between Al2O3-Fe2O3-SiO2 after Schellmann [19]

The classification diagram of Boulangé [20] shows that most of the bauxitic samples from the Parawi plateau are located in the fields of bauxite (PrwBF111, PrwBF090, PrwBF091, PrwBF144, PrwBF150 and PrwBF161) and ferruginous bauxite (PrwBF080, PrwBF100, PrwBF102, PrwBF104, PrwBF105, PrwBF110, PrwBF120, PrwBF151, and PrwBF152). Some bauxite samples (PrwBF013, PrwBF051, PrwBF104 and PrwBF143) are positioned in the transition zone between the fields of bauxite and ferruginous bauxite, reflecting a gradual evolution between these two facies. Finally, a single sample of bauxite (PrwBF140) is found in the kaolinite field (Figure 9).

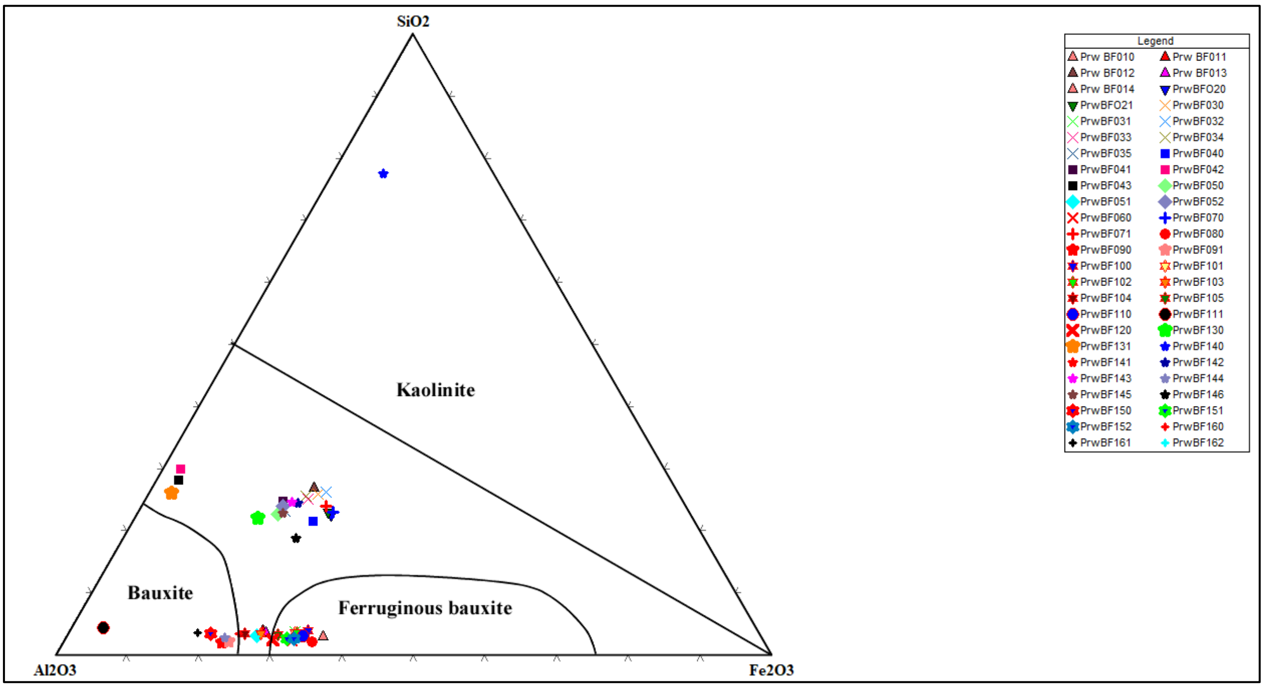

Figure 9 Triangular diagram between Al2O3-Fe2O3-SiO2 after Boulangé [20]

The geochemical diagram of Beauvais [21] and Tardy [22] clearly illustrates the different evolutionary trajectories of the samples from the Parawi plateau under the effect of bauxitization processes (Figure 10). A single sample of bauxite (PrwBF140) is located in the area corresponding to the preservation of kaolinite, reflecting a relative conservation of this mineral during alteration. Conversely, some bauxite samples (PrwBF012, PrwBF030, PrwBF032 PrwBF033, PrwBF034, PrwBF040, PrwBF041, PrwBF042, PrwBF043, PrwBF050, PrwBF052, PrwBF070, PrwBF071, PrwBF130 and PrwBF142), are placed in the field of ferruginous enrichment, associated with an increased concentration of Fe2O3, indicating a marked trend towards the ferruginization of laterite materials (Figure 10).

Finally, several samples (PrwBF010, PrwBF080, PrwBF090, PrwBF091, PrwBF110, PrwBF120, PrwBF150, PrwBF151, PrwBF152, PrwBF160, PrwBF161 among others) follow the trajectory of kaolinite destruction, a process intimately linked to clay mineral dehydration (Figure 10). This evolution leads to the formation of bauxite rich in alumina and iron. The entire diagram thus highlights the diversity of geochemical paths taken by the samples, ranging from the simple preservation of kaolinite to its complete transformation into ferruginous bauxitic facies [2], [3], [11], [15], [16], [17], [18].

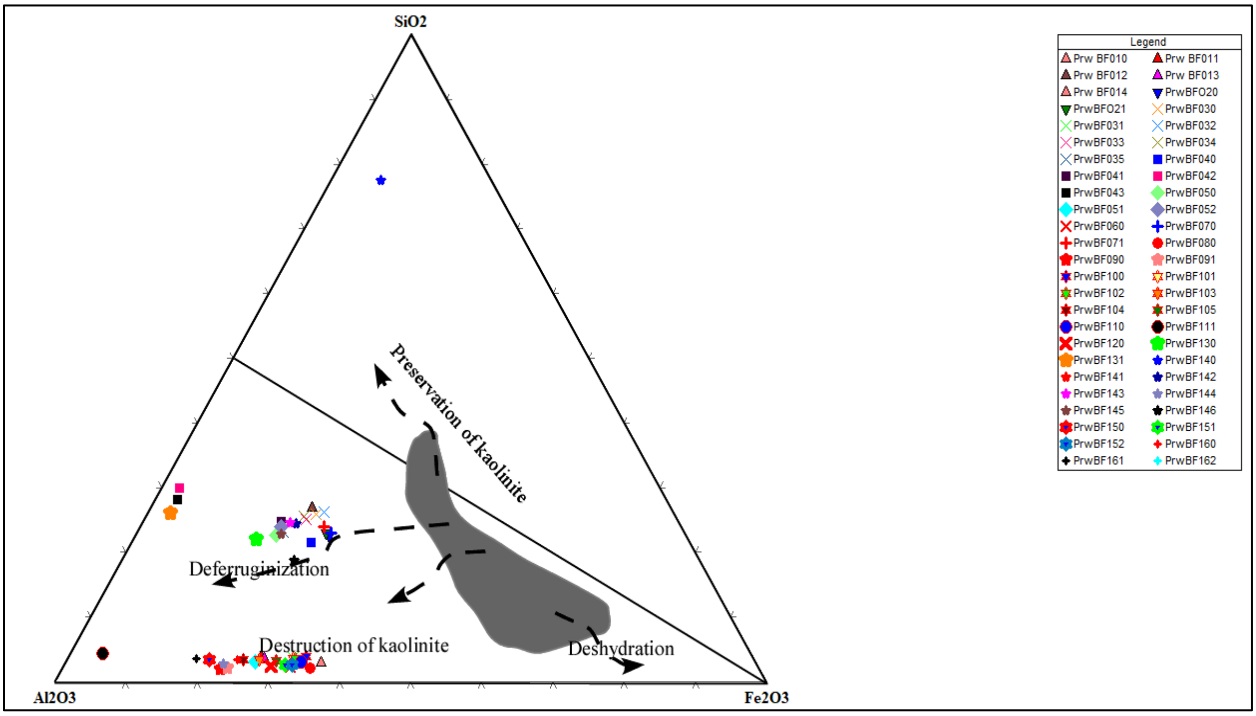

Figure 10 Triangular diagram between Al2O3-Fe2O3-SiO2 after Beauvais [21] and Tardy [22]

To better understand the geochemical behavior of major elements, we have created correlation diagrams between Al2O3 on one hand, and SiO2, Fe2O3 and TiO2 on the other (Figure 11). The results show that the TiO2 and Fe2O3 contents decrease when the Al2O3 content increases. This relationship reflects a negative correlation: the more alumina is enriched, the more titanium minerals (rutile, anatase) and iron-bearing minerals (hematite, goethite, alumogoethite) regress in favor of aluminous phases such as gibbsite and boehmite [22], [23], [24], [25]. In the same way, the correlation diagram between SiO2 and Al2O3 highlights a weak negative correlation. This means that when the silica (mainly carried by quartz and kaolinite) decreases, the proportion of alumina (gibbsite, boehmite) increases. This behavior suggests that bauxite from the Parawi plateau has a tendency to pure alumina enrichment and silica depletion, which is a major asset for its exploitation, because a high Al2O3 content associated with a low proportion of SiO2 is particularly favorable to the production of aluminum (Figure 12) [22], [23], [24], [25].

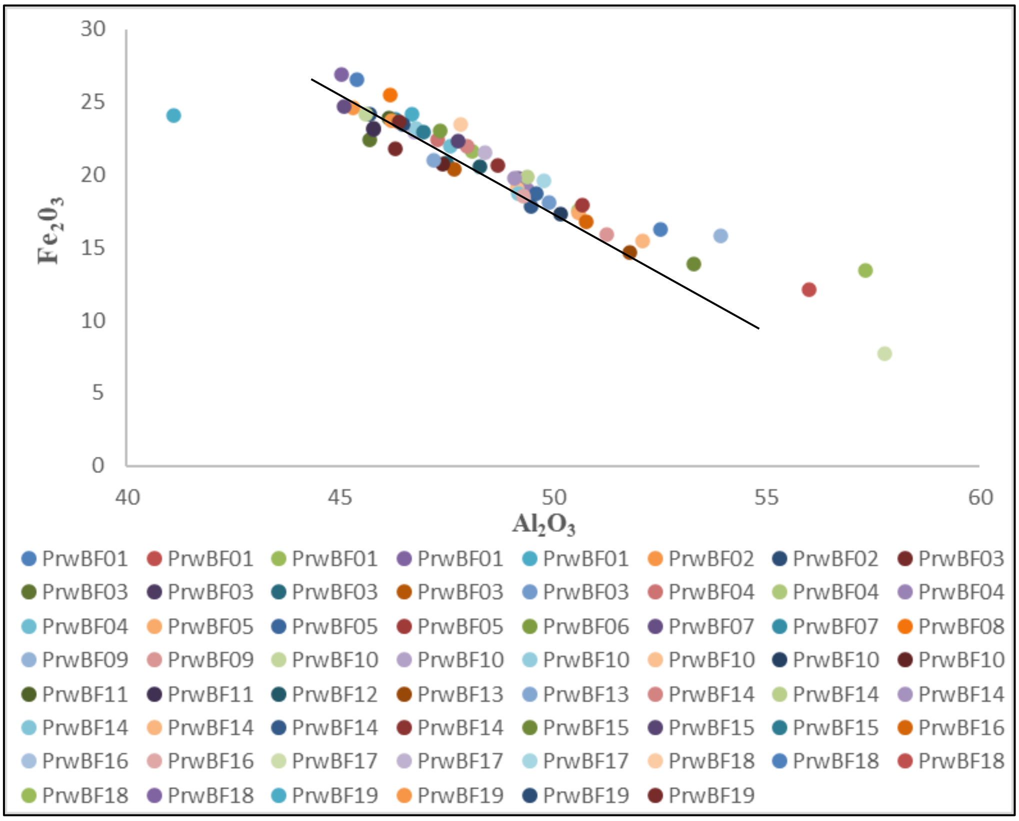
Fe2O3
Al2O3
30
25
20
15
10
5
0
40
45
50
55
60
PrwBF01 PrwBF01 PrwBF01 PrwBF01 PrwBF01 PrwBF02 PrwBF02 PrwBF03
PrwBF03 PrwBF03 PrwBF03 PrwBF03 PrwBF03 PrwBF04 PrwBF04 PrwBF04
PrwBF04 PrwBF05 PrwBF05 PrwBF05 PrwBF06 PrwBF07 PrwBF07 PrwBF08
PrwBF09 PrwBF09 PrwBF10 PrwBF10 PrwBF10 PrwBF10 PrwBF10 PrwBF10
PrwBF11 PrwBF11 PrwBF12 PrwBF13 PrwBF13 PrwBF14 PrwBF14 PrwBF14
PrwBF14 PrwBF14 PrwBF14 PrwBF14 PrwBF15 PrwBF15 PrwBF15 PrwBF16
PrwBF16 PrwBF16 PrwBF17 PrwBF17 PrwBF17 PrwBF18 PrwBF18 PrwBF18
PrwBF18 PrwBF18 PrwBF19 PrwBF19 PrwBF19 PrwBF19

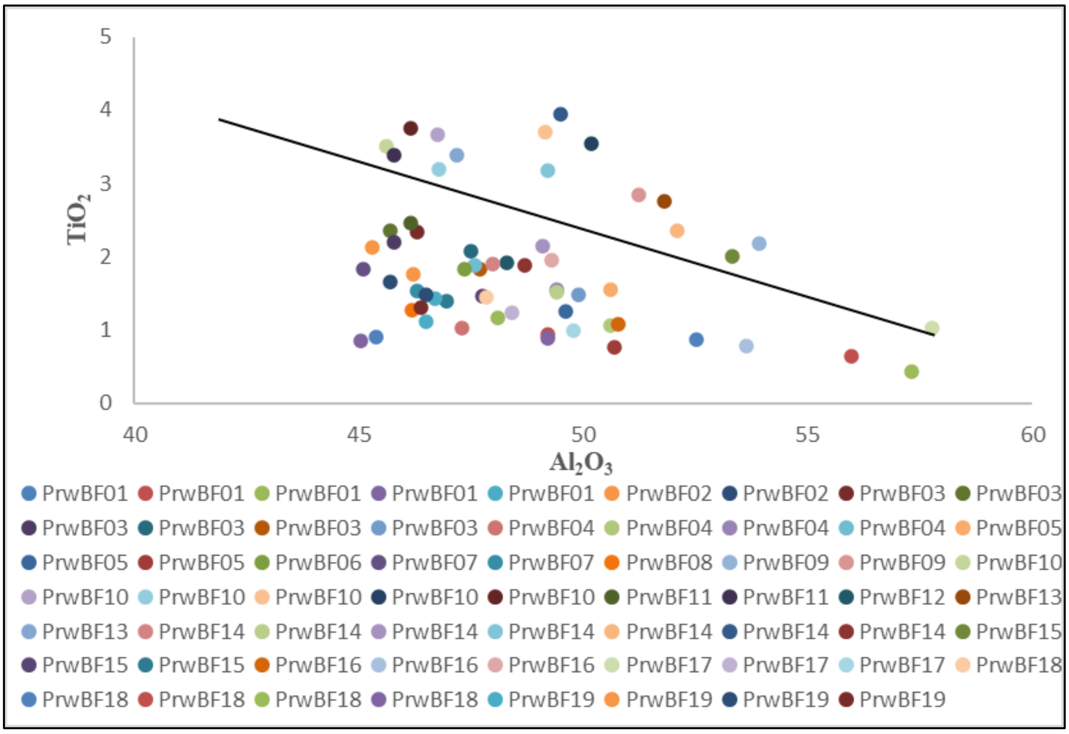
TiO2
Al2O3
5
4
3
2
1
0
40
45
50
55
60
PrwBF01 PrwBF01 PrwBF01 PrwBF01 PrwBF01 PrwBF02 PrwBF02 PrwBF03 PrwBF03
PrwBF03 PrwBF03 PrwBF03 PrwBF03 PrwBF04 PrwBF04 PrwBF04 PrwBF04 PrwBF05
PrwBF05 PrwBF05 PrwBF06 PrwBF07 PrwBF07 PrwBF08 PrwBF09 PrwBF09 PrwBF10
PrwBF10 PrwBF10 PrwBF10 PrwBF10 PrwBF10 PrwBF11 PrwBF11 PrwBF12 PrwBF13
PrwBF13 PrwBF14 PrwBF14 PrwBF14 PrwBF14 PrwBF14 PrwBF14 PrwBF14 PrwBF15
PrwBF15 PrwBF15 PrwBF16 PrwBF16 PrwBF16 PrwBF17 PrwBF17 PrwBF17 PrwBF18
PrwBF18 PrwBF18 PrwBF18 PrwBF18 PrwBF19 PrwBF19 PrwBF19 PrwBF19

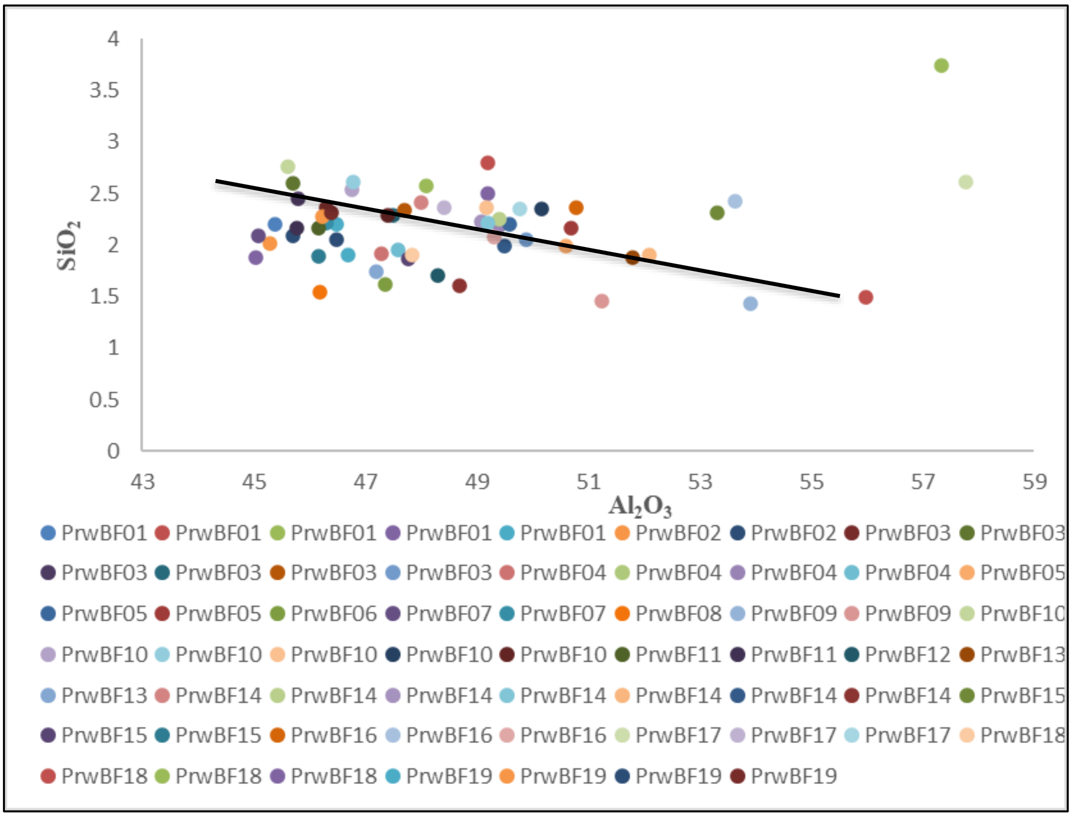

Figure 11 Correlation diagram of Fe2O3, TiO2 and SiO2 as a function of Al2O3

5. Conclusion

The geological characterization of the bauxitic deposit of Parawi highlights three main types of bauxite: lateritic bauxite, resulting from both the alteration of the Devonian aleuro-argillite and the Mesozoic dolerite; sedimentary bauxite and chemogenic bauxite, formed by the chemical redistribution of elements at the base of lateritic horizons.

Among the latter, one distinguishes gelled bauxites, which still retain certain textural and structural characteristics of the source rocks, and gélomorphic bauxites, completely transformed by the processes of concentration and reorganization of aluminous material.

From the mineralogical point of view, these bauxites are made up overwhelmingly of gibbsite (about 91% by volume), accompanied by lower proportions of boehmite and aluminous goethite. Accessory minerals such as rutile, kaolinite, hematite and quartz appear in minor amounts.

Correlation diagrams show interesting trends: the TiO2 and Fe2O3 contents decrease when the Al2O3 content increases, revealing a negative correlation. This reflects a regression of titanium minerals (rutile, anatase) and ferruginous (hematite, goethite, alumogoethite), along with an increase in aluminous phases such as gibbsite and boehmite. In the same way, the correlation between SiO2 and Al2O3 remains negative but weaker: as quartz and kaolinite decrease, alumina increases. This behavior indicates that the bauxite from Parawi is generally rich in pure alumina and poor in silica, a characteristic favorable to aluminum production

X-ray diffraction (XRD) analyses and thin-plate observations confirm these results: bauxites are dominated by gibbsite, and their geochemical composition reveals up to 68 wt% of Al2O3, associated with low proportions of Fe2O3, TiO2 and SiO2.

Finally, the ternary diagrams of the major elements make it possible to specify the evolution of the deposit: on one hand, they show that the process of bauxitisation is accompanied by the gradual destruction of kaolinite ; on the other hand, they reveal that the majority of bauxites, as well as the ferruginous laterites and the ferriplantites, are strongly laterized, even if some samples still show a lower degree of laterization. Overall, we observe that the contents of quartz, kaolinite and hematite decrease as gibbsite is enriched, confirming the evolution towards high quality aluminous bauxite.

Compliance with ethical standards

Disclosure of conflict of interest

No conflict of interest to be disclosed. Yes, there is no conflict of interest between the different authors.

References

[1] A. Abedini, A. A. Calagari, et K. Mikaeili, « Geochemical characteristics of laterites: the Ailibaltalu deposit, Iran », Maden Tetk. Ve Arama Derg., vol. 148, no 148, p. 69-84, 2014.

[2] M. Sidibe et M. G. Yalcin, « Petrography, mineralogy, geochemistry and genesis of the Balaya bauxite deposits in Kindia region, Maritime Guinea, West Africa », J. Afr. Earth Sci., vol. 149, p. 348-366, janv. 2019, doi: 10.1016/j.jafrearsci.2018.08.017.

[3] A. K. Diallo, M. S. M. Conte, O. B. Kaba, A. Soumah, et M. Camara, « Petrological and Statistical Studies of the Limbiko Bauxite Deposit, Republic of Guinea », Int. J. Geosci., vol. 14, no 04, p. 351-376, 2023, doi: 10.4236/ijg.2023.144020.

[4] Statista, « Principaux pays producteurs de bauxite 2013-2019 | Statista ». Consulté le: 15 mars 2021. [En ligne]. Disponible sur: https://fr.statista.com/statistiques/565292/principaux-pays-de-la-production-mondiale-miniere-de-bauxite/

[5] « Potentiel minéral – Ministère des Mines et de la Géologie ». Consulté le: 30 août 2025. [En ligne]. Disponible sur: https://mines.gov.gn/potentiel-mineral/

[6] M. Esterle et J.-P. Lajoinie, « BAUXITES - Encyclopædia Universalis », Universalis. Consulté le: 15 mars 2021. [En ligne]. Disponible sur: https://www.universalis.fr/encyclopedie/bauxites/

[7] V. I. Mamedov, Y. V. Boufeev, et Y. A. Nikitine, Géologie de la République de Guinée. Ministère des Mines et de la Géologie de la République de Guinée, 2010.

[8] V. I. Mamedov, V. Tokarlikov, M. Seredkin, et O. Chaplyguine, « Résultats de la première phase d'exploration sur le territoire de la Concession HALCO », GEOCONSULT Ltd, Boké, 1998.

[9] V. I. Mamedov et al., « Résultats de la prospection préliminaire (150m x150m) et études spéciales éffectuées sur les gisements de Kooni (bowal 5), Dalagala (bowal 6), Tiapikoré-Nord (bowal 8 Nord), Fello Maoulé (bowal 9), Kagnaka (bowal 25), Yaladanè (bowal 29) ET Limbiko (bowal 30) », GEOPROSPECTS Ltd, Boké, août 2005.

[10] V. I. Mamedov, Y. V. Bouffev, et Y. A. Nikitine, « Banque de données sur les gisements et indices des minéraux utiles », Min Mines Géologie Rép Guinée GEOPROSPECTS Ltd, 2010.

[11] V. I. Mamedov, A. A. Chausovb, E. A. Okonovb, M. A. Makarovaa, et N. M. Boevac, « The World's Largest Fouta Djallon–Mandingo Bauxite Province (West Africa): Part I. Background », Geol. ORE Depos., vol. 62, no 2, p. 163-176, 2020.

[12] V. I. Mamedov, M. A. Makarova, et V. A. Zaitsev, « The World's Largest Fouta Djallon–Mandingo Bauxite Province (West Africa): Part III. The Influence of Geomorphic Factors and the Age of Relief on the Spatial Distribution, Size, and Quality of Bauxite Deposits », Geol. Ore Depos., vol. 64, no Suppl 1, p. 15-42, 2022.

[13] A. Diallo, A. L. Diallo, et I. Diallo, « «Géologie et projet de prospection d'etaillées du gisement bauxitique de Boullérè (Bowal 05) CBG », INSTITUT SUPERIEUR DES MINES ET GEOLOGIE DE BOKE, BOKE, 2010.

[14] G. J. J. Aleva, « Laterites: concepts, geology, morphology and chemistry. », in The Corlat Handbook, 1re éd., vol. 1, in CORLAT Technical Publication, vol. 1. , Brussels, Belgium: International Soil Reference and Information Centre (ISRIC), 1994, p. 8-21.

[15] A. Abedini et A. A. Calagari, « Geochemical characteristics of Kanigorgeh ferruginous bauxite horizon, West-Azarbaidjan province, NW Iran », Period. Mineral., vol. 82, no 1, 2013, doi: http://dx.doi.org/10.2451/2013PM0001.

[16] M. Z. Abzalov et J. Bower, « Geology of bauxite deposits and their resource estimation practices », Appl. Earth Sci., vol. 123, no 2, p. 118-134, juin 2014, doi: 10.1179/1743275814Y.0000000046.

[17] P. G. Bhukte et al., « Geochemical, Mineralogical and Petrological Characteristics of Lateritic Bauxite Deposits formed on Deccan Trap Basalt with Reference to High-level and Coastal (low level) Deposits of Maharashtra », J. Geol. Soc. India, vol. 95, no 6, p. 587-598, juin 2020, doi: 10.1007/s12594-020-1485-1.

[18] B. Bogatyrev et V. Zhukov, « Bauxite provinces of the world », Geol. Ore Depos., vol. 51, p. 339-355, oct. 2009, doi: 10.1134/S1075701509050018.

[19] W. Schellmann, « On the geochemistry of laterites », Chem. Erde, vol. 45, p. 39-52, 1986.

[20] B. Boulangé, G. Bouzat, et M. Pouliquen, « Mineralogical and geochemical characteristics of two bauxitic profiles, Fria, Guinea Republic », Miner. Deposita, vol. 31, no 5, p. 432-438, juill. 1996, doi: 10.1007/BF00189190.

[21] A. Beauvais, « Paléoclimats et dynamique d'un paysage cuirassé du centrafrique : morphologie, pétrologie et géochimie », These de doctorat, Poitiers, 1991. Consulté le: 28 janvier 2021. [En ligne]. Disponible sur: https://www.theses.fr/1991POIT2333

[22] Y. Tardy, J.-L. Boeglin, et C. Roquin, « Petrological and geochemical classification of bauxites and their associated iron-rich laterites », 1997.

[23] J. Gu, Z. Huang, H. Fan, Z. Jin, Z. Yan, et J. Zhang, « Mineralogy, geochemistry, and genesis of lateritic bauxite deposits in the Wuchuan–Zheng'an–Daozhen area, Northern Guizhou Province, China », J. Geochem. Explor., vol. 130, p. 44-59, juill. 2013, doi: 10.1016/j.gexplo.2013.03.003.

[24] G. Komlóssy, C. van Deursen, et B. E. Raahauge, « Bauxite: Geology, Mineralogy, Resources, Reserves and Beneficiation », in Smelter Grade Alumina from Bauxite, Springer, 2022, p. 19-132.

[25] X. Liu, Q. Wang, Q. Zhang, Y. Feng, et S. Cai, « Mineralogical characteristics of the superlarge Quaternary bauxite deposits in Jingxi and Debao counties, western Guangxi, China », J. Asian Earth Sci., vol. 52, p. 53-62, 2012.